The Plant Cell, Vol. 17, 691–704, March 2005, www.plantcell.org © 2005 American Society of Plant Biologists

CORONA, a Member of the Class III Homeodomain Leucine Zipper Gene Family in Arabidopsis, Regulates Stem Cell Specification and Organogenesis [W]

Kirsten A. Green, Michael J. Prigge, Rebecca B. Katzman,[1] and Steven E. Clark[2]

Department of Molecular, Cellular, and Developmental Biology, University of Michigan, Ann Arbor, Michigan 48109-1048

Organogenesis at the shoot meristem requires a delicate balance between stem cell specification and differentiation. In *Arabidopsis thaliana*, *WUSCHEL* (*WUS*) is a key factor promoting stem cell identity, whereas the *CLAVATA* (*CLV1*, *CLV2*, and *CLV3*) loci appear to promote differentiation by repressing *WUS* expression. In a screen for mutations modifying *clv1* mutants, we have identified a novel regulator of meristem development we term *CORONA* (*CNA*). Whereas *cna* single mutant plants exhibit subtle defects in meristem development, *clv cna* double mutants develop massively enlarged apices that display early loss of organogenesis, misexpression of *WUS* and *CLV3*, and eventual differentiation of the entire apex. The *CNA* gene was isolated by positional cloning and found to encode a class III homeodomain Leu zipper protein. A missense mutation resulting in the dominant-negative *cna-1* allele was identified in a conserved domain of unknown function, and a likely null allele was shown to display a similar but weaker phenotype. *CNA* is expressed in developing vascular tissue, diffusely through shoot and flower meristems, and within developing stamens and carpels. Our analysis of *WUS* expression in wild-type, *clv*, and *clv cna* plants revealed that, contrary to current models, *WUS* is neither necessary nor sufficient for stem cell specification and that neither *WUS* nor *CLV3* is a marker for stem cell identity. We propose that *CNA* functions in parallel to the *CLV* loci to promote organ formation.

INTRODUCTION

A central feature of plant development is the continuous generation of organs throughout the plant's lifespan. The capacity to generate new above-ground organs post-embryonically is a property of shoot meristems. Within shoot meristems reside stem cells that are maintained at a constant number while giving rise to organ primordia and ultimately all of the differentiated cells of organs and tissues (Steeves and Sussex, 1989). In this way, shoot meristems have the capacity to balance perpetual differentiation of cells while replenishing the pool of undifferentiated, pluripotent cells.

Genetic screens have identified several key regulators of shoot meristem development (Barton and Peothig, 1993; Clark et al., 1993; Laux et al., 1996; Pogany et al., 1998; Yu et al., 2000). The *WUSCHEL* (*WUS*) gene encodes a homeodomain protein, which is an important regulator of stem cell identity (Mayer et al., 1998; Schoof et al., 2000). Loss-of-function *wus* mutants fail to organize functional shoot meristems. After germination, *wus* mutants sporadically generate adventitious shoots, which form only a few organs before termination (Endrizzi et al., 1996; Laux et al., 1996). Expression of *WUS* within the meristem appears to be sufficient for establishing stem cell identity. When *WUS* was ectopically expressed, transgenic seedlings accumulate undifferentiated stem cells (Schoof et al., 2000).

Three *CLAVATA* genes (*CLV1*, *CLV2*, and *CLV3*) promote the differentiation of stem cells. Loss-of-function *clv1*, *clv2*, and *clv3* mutants accumulate undifferentiated cells in shoot and floral meristems, resulting in meristems that are significantly larger than the wild type and in flowers with increased numbers of floral organs (Clark et al., 1993, 1995; Jeong et al., 1999). The *CLV1*, *CLV2*, and *CLV3* loci encode signal transduction components: a receptor kinase (Clark et al., 1997), a receptor-like protein (Jeong et al., 1999), and a small secreted protein (Fletcher et al., 1999), respectively.

WUS is a key target of the *CLV* signal transduction pathway (Brand et al., 2000; Schoof et al., 2000). In wild-type plants, the domain of *WUS* expression is normally restricted to a small, centrally located subset of cells beneath the three outermost cell layers (Mayer et al., 1998; Schoof et al., 2000). In *clv3* mutant meristems, the *WUS* expression domain expands laterally and apically into the topmost cells of the L3 layer (Brand et al., 2000; Schoof et al., 2000). Conversely, plants overexpressing *CLV3* recreate the Wus$^-$ phenotype and do not appear to express *WUS* mRNA (Brand et al., 2000), indicating that the CLV signaling pathway limits stem cell number by restricting the size of the *WUS* expression domain.

Overexpression of *WUS* through promoter fusions can also lead to ectopic stem cell accumulation (Schoof et al., 2000).

[1] Current address: Department of Microbiology/Immunology, Northwestern University Medical School, 303 East Chicago Ave., Ward 6-260, Chicago, IL 60611.

[2] To whom correspondence should be addressed. E-mail clarks@umich.edu; fax 734-647-0884.

The author responsible for distribution of materials integral to the findings presented in this article in accordance with the policy described in the Instructions for Authors (www.plantcell.org) is: Steven E. Clark (clarks@umich.edu).

[W] Online version contains Web-only data.

Article, publication date, and citation information can be found at www.plantcell.org/cgi/doi/10.1105/tpc.104.026179.

Interestingly, transcripts of *CLV3* are found on the periphery of stem cell masses formed by *WUS* overexpression, whereas in the meristems of wild-type plants, *CLV3* expression is restricted to the center of the shoot meristem (Fletcher et al., 1999; Schoof et al., 2000). These expression analyses indicate that while the CLV signaling pathway targets *WUS* and restricts its activity, *WUS* activity is also sufficient to induce transcription of *CLV3*. This regulatory feedback loop may act to maintain strict control of the number of stem cells.

In this study, we describe a novel regulator of shoot meristem development, *CORONA*. We show that *CNA* encodes a class III homeodomain Leu zipper (HD-Zip III) transcription factor that plays an important role in the maintenance of stem cell function. Members of this gene family, which also includes the *REVOLUTA* (*REV*), *PHABULOSA* (*PHB*), *PHAVOLUTA* (*PHV*), and *ATHB8* genes, have previously been implicated in several aspects of *Arabidopsis thaliana* development, including meristem and organ development (Talbert et al., 1995; McConnell and Barton, 1998; Zhong and Ye, 1999; Baima et al., 2001; McConnell et al., 2001; Otsuga et al., 2001; Zhong and Ye, 2001; Prigge et al., 2005). In addition, we show that *WUS* expression might not be necessary for stem cell specification in *clv3-2* mutants. The latter finding suggests that a *WUS* independent pathway exists and is involved in specifying stem cell identity at certain stages in development. Furthermore, we demonstrate that *WUS* and *CLV3* expression can be found in differentiated tissues.

RESULTS

Isolation of a *cna* Mutant

An ethyl methanesulfonate mutagenesis was performed on *clv1-1* mutant seeds to identify enhancers and/or suppressors of the Clv$^-$ phenotype (Pogany et al., 1998). A strong modifier of *clv1-1* plants was identified in this screen (pce5). The enhancing mutation was backcrossed to Landsberg *erecta* (L*er*) and isolated (see Methods). The modifier acted as a single, nuclear trait in all crosses. When combined with strong *clv* alleles, the enhancer led to the development of corona or ring-like meristems, leading us to name the gene *CORONA* (*CNA*).

cna-1 plants appeared superficially wild type in phenotype. Scanning electron microscopy analysis of *cna-1* shoot meristems revealed that the meristems of 12-d-old *cna-1* plants are significantly larger than wild-type meristems (see Supplemental Figure 1 online; Table 1). The effect, if any, of *cna-1* on shoot meristem size in 24-d-old plants is reduced compared with earlier developmental time points (Table 1).

Table 1. Twelve-Day-Old *cna-1* Meristems Are Larger Than Those in the Wild Type

Genotype	Day 12	Day 24
L*er*	55.6 ± 0.99 ($n = 5$)	57.3 ± 1.48 ($n = 10$)
cna-1	72.7 ± 1.72 ($n = 10$)	61.1 ± 1.67 ($n = 15$)

The size of the shoot apical meristem (in micrometers) of *cna-1* and L*er* plants at 12 and 24 d old was determined. The mean ± standard error is presented. The difference between means is statistically significant on day 12 (*t* test, $P < 0.0001$) but is less statistically significant on day 24 (*t* test, $P = 0.1$).

Genetic interactions with *clv* mutations

Double mutants were generated between *cna-1* and various *clv1*, *clv2*, and *clv3* alleles. The effect of *cna-1* on *clv* mutant phenotypes and whether *cna* was recessive or incompletely dominant depended on the severity of the *clv* allele. When combined with a phenotypically weak *clv* allele, such as *clv1-7*, *cna-1* enhanced the Clv$^-$ phenotype in terms of shoot meristem size (see Supplemental Figures 2A and 2B online; Table 2). When *cna-1* was combined with *clv* alleles of intermediate severity, such as *clv1-1* and *clv2-1*, *cna-1* was also recessive but led to the development of more severe phenotypes. These included dramatic enlargement of shoot meristem size, the eventual loss of organ formation at the apex, and frequent differentiation of apical cells followed by organ formation in the center of the shoot meristem (leading to a ring-like or corona meristem) (see Supplemental Figure 2 online; Figures 1I and 1J, Table 2).

The *cna-1* double mutants with the strong *clv* alleles *clv1-4*, *clv1-8*, *clv3-1*, and *clv3-2* exhibited the most dramatic phenotypes, and these double mutants were analyzed in the greatest detail. In contrast with other backgrounds, *cna-1* was incompletely dominant and displayed dominant-negative characteristics in the phenotypically stronger *clv1-4*, *clv1-8*, *clv3-1*, and *clv3-2* backgrounds (Tables 2 and 3; see Supplemental Table 2 online). The *clv cna-1* double mutants with these *clv* alleles developed shoot meristems that were enlarged in comparison with *clv* meristems, even at early stages of vegetative development (see Supplemental Figure 2 online; Figures 1A to 1C and 2A to 2F, Tables 2 and 3). Early in development, *clv3-2 cna-1* plants had visible, enlarged meristems and also occasionally lacked identifiable young organ primordia around portions of the periphery of the shoot meristem (Figures 1C, 1E, and 2A to 2D). This loss-of-organogenesis phenotype exhibited strong variation in expressivity early in development, although at later stages we consistently observed apices with older primordia but not younger primordia (see Supplemental Figure 2 online; Figures 1 and 2). The loss of organ formation was not always uniform around the periphery of the shoot meristem (Figures 1 and 2). Moreover, a plant that had initiated no or few leaves during vegetative development could later initiate flower primordia (Figures 2B to 2D).

Along with the loss of organogenesis in *clv3-2 cna-1* plants, we also observed that the entire apices of *clv3-2 cna-1* plants eventually differentiated into organs. Subtle changes in the topography of the shoot apical meristems of *clv3-2 cna-1* plants ~8 d old were observed by scanning electron microscopy, with an indentation appearing in the center of the meristem (Figures 1A and 1B). Starting at approximately day 15, carpeloid and filamentous organs often formed in the center of the *clv3-2 cna-1* meristems (Figures 1F to 1H), leaving a ring of more meristem-like tissue. *clv3-2 cna-1* apices eventually differentiated across the entire apical region (Figures 1F to 1J).

Key regulators of meristem development often affect both shoot and flower meristem function. However, we detected no

Table 2. *cna* Mutations Enhance *clv* Shoot Meristem Sizes

Genotype	Shoot Meristem Size (μm)[a]	Age (d)[b]	*n*[c]
clv2-1	58 ± 2.5[d]	13	12
clv2-1 cna-1/cna-1	109 ± 16.6	13	12
clv3-2	163 ± 11.1[e]	13	18
clv3-2 cna-1/+	196 ± 9.1	13	18
clv3-2 cna-1/cna-1	276 ± 9.3	13	32
clv3-2 cna-2/cna-2	223 ± 12.1	13	16
clv1-7	71 ± 2.8[f]	15	8
clv1-7 cna-1/cna-1	95 ± 2.1	15	8

[a] Values represent the mean shoot apical meristem diameter ± standard error (see Methods).
[b] Age indicates the days after germination plants were collected.
[c] *n* indicates the number of measurements used to determine size.
[d] The mean meristem diameter for *clv2-1* is significantly different from that of *clv2-1 cna-1* plants (*t* test, $P < 0.01$).
[e] The mean meristem diameter for *clv3-2* is significantly different from that of *clv3-2 cna-1/CNA* plants ($P = 0.03$), *clv3-2 cna-1* plants (*t* test, $P < 0.01$), and *clv3-2 cna-2* plants ($P < 0.01$).
[f] The mean meristem diameter for *clv1-7* is significantly different from that of *clv1-7 cna-1* plants (*t* test, $P < 0.01$).

consistent effect of *cna* mutations on flower meristem development or flower organ number either in *cna* single mutants or in combination with *clv3-2* (Table 4). *clv cna* lateral shoot meristems recapitulated the defects observed in the *clv cna* shoot apical meristems, albeit to a lesser degree (data not shown).

clv cna plants often developed enlarged inflorescence stems. To determine if defects in stem vascular patterning were associated with this phenotype, phloroglucinol- and toluidine blue–stained cross sections of *clv3-2 cna-1* inflorescence stems were compared with those from *clv3-2* single mutants. Although *clv3-2* stems have an increased number of vascular bundles compared with wild-type plants, all of these bundles are located around the periphery of the stem as is observed in the wild type (Figure 2G; data not shown). *clv3-2 cna-1* plants, on the other hand, form ectopic vascular bundles in the center of the stem (Figure 2H). The *clv3-2 cna-1* ectopic bundles exhibited an apparent inside-out morphology, with xylem surrounding phloem (Figure 2I). The ectopic bundles would occasionally form a second ring of vascular bundles in the center of the stem (Figure 2H).

In summary, the *cna-1* mutation led to severe disruptions in meristem size, organogenesis, and stem cell specification, particularly in genetic backgrounds lacking CLV signaling. There was variable expressivity of Cna^- phenotypes among *clv cna-1* plants. The variable Cna^- expressivity was consistently observed in crosses to several genetic ecotypes and among all isolates of such crosses, suggesting it was not the result of segregating genetic polymorphisms (data not shown).

wus and *stm* Are Epistatic to *cna-1*

WUS and *STM* are key regulators of meristem development, but exhibit different genetic interactions with *clv* mutants. *wus* is epistatic to *clv* (Laux et al., 1996; Schoof et al., 2000; Yu et al., 2003), and *stm* is additive with *clv* (Clark et al., 1996). Genetic interactions among *cna-1*, *stm*, and *wus* were investigated to refine the placement of *CNA* within the hierarchy of genes regulating meristem development. Because *cna-1* induced the most dramatic phenotypic effects in the *clv3-2* background, we used the *clv3-2* background to assay these genetic interactions. *clv3-2 cna-1 wus-1* triple mutant plants appeared identical to *clv3-2 wus-1* and *wus-1* plants in terms of overall plant morphology and lack of meristem activity (Figures 3A and 3B; data not shown), indicating that *wus-1* was epistatic to *cna-1* in a *clv3-2* background.

We examined genetic interactions between *SHOOTMERISTEMLESS* (*STM*) and *CNA*. *STM* is a member of the KNOTTED-like homeobox gene family (Long et al., 1996), thought to be important for maintaining cells in an undifferentiated state by repressing differentiation factors (Byrne et al., 2000, 2002). Strong loss-of-function *stm* mutants fail to establish the embryonic shoot meristem and lack postembryonic organ formation (Barton and Poethig, 1993; Endrizzi et al., 1996). Whereas *clv* mutants partially repress this phenotype (Clark et al., 1996), *clv3-2 cna-1 stm-1* mutants were identical in phenotype to *stm-1* single mutants (Figures 3C and 3D), indicating that *stm-1* is epistatic to *clv3-2 cna-1*.

Identification of *CNA*

We used a map-based cloning strategy to isolate the *CNA* gene. *CNA* was mapped to chromosome 1, within a 10-centimorgan region delimited by simple sequence length polymorphism markers ciw1 and nga128 (Bell and Ecker, 1994; Lukowitz et al., 2000). Using new cleaved-amplified polymorphic sequence (CAPS) markers, the location of *CNA* was narrowed down to a region spanning 162 kb (Figure 4A). Among the annotated genes in the 162-kb region, we noted *At1g52150*, which encodes a HD-Zip III putative transcription factor, previously referred to as *ATHB15* (Baima et al., 2001; Ohashi-Ito and Fukuda, 2003). A nucleotide change resulting in an Ala-to-Val amino acid substitution at residue 606 (A606V) was discovered at this locus in the *cna-1* genome (Figure 4B). This position is within a domain of unknown function conserved within the gene family (Figure 4C; data not shown).

To confirm that *At1g52150* was indeed *CNA*, we obtained an allele in the Columbia background, *cna-2*, with a T-DNA insertion in the second exon of *At1g52150* (Figure 4B; Prigge et al., 2005). *cna-2* single mutant plants appeared superficially wild type (Prigge et al., 2005). The *clv3-2 cna-2* double mutants exhibited a phenotype similar to, although less severe than, that of *clv3-2 cna-1* plants (Figure 2K, Tables 2 and 3). When assayed for RNA accumulation by RT-PCR, we found similar accumulation of *CNA* and *cna-1* transcripts, but no accumulation of full-length *cna-2* transcripts (see Supplemental Figure 3 online). Because *cna-1* contained the entire coding sequences, yet exhibited both a stronger phenotype than *cna-2* and an incompletely dominant effect in strong *clv* mutant backgrounds, we propose that *cna-1* is dominant-negative, which is further supported by *cna-1/cna-2* transheterozygous phenotypes (Table 3; see Supplemental Table 3 online). Interestingly, the *rev-3* allele has a Thr-to-Ile amino acid substitution (T608I) at the position equivalent to that of the

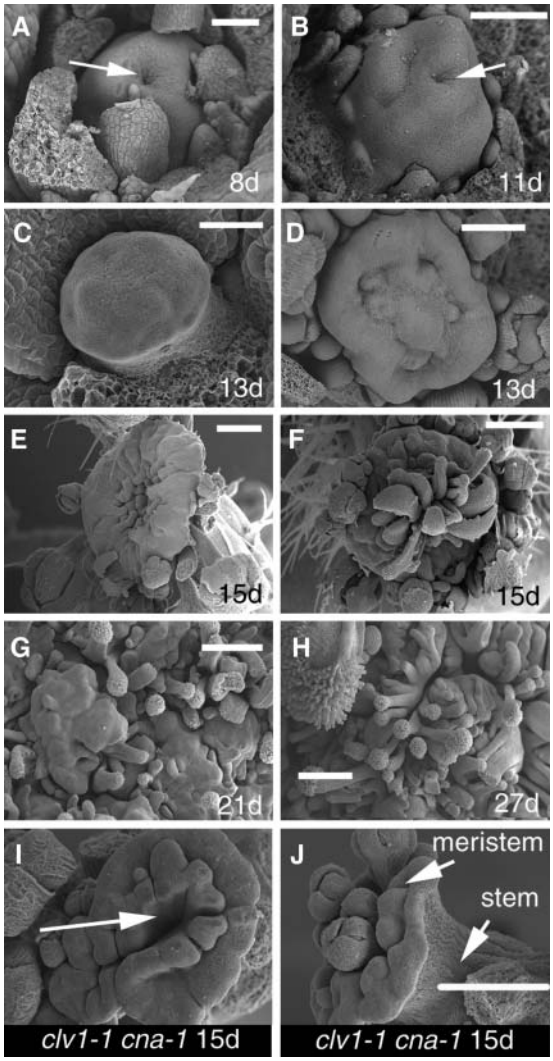

Figure 1. Apex Differentiation in *clv cna-1* Meristems.

Scanning electron micrographs of *clv3-2 cna-1* (**[A]** to **[H]**) and *clv1-1 cna-1* (**[I]** and **[J]**) shoot apices. Bars = 50 μm in **(A)**, 100 μm in **(B)** to **(D)**, and 250 μm in **(E)** to **(J)**. **(I)** and **(J)** are shown at the same magnification.
(A) Apex from an 8-d-old *clv3-2 cna-1* plant. Arrow indicates central defect in the meristem.
(B) Apex from an 11-d-old *clv3-2 cna-1* plant. Arrow indicates central defect in the meristem.
(C) Apex from a 13-d-old *clv3-2 cna-1* plant. Note the lack of organ primordia around the periphery.
(D) Apex from a 13-d-old *clv3-2 cna-1* plant. Note the tissue buckling across the center.
(E) Apex from a 15-d-old *clv3-2 cna-1* plant. Note the lack of younger primordia around most of the periphery.
(F) Apex from a 15-d-old *clv3-2 cna-1* plant. Note the large carpeloid organs formed in the center of the meristem.
(G) A portion of the apex from a 21-d-old *clv3-2 cna-1* plant. Note the extensive initiation of filamentous organs with stigmatic tissues at their tips.
(H) A portion of the apex from a 27-d-old *clv3-2 cna-1* plant. Note the absence of any meristem-like region.
(I) Apex from a 15-d-old *clv1-1 cna-1* plant. Note the ectopic organs in the center of the meristem (arrow).
(J) Apex from a 15-d-old *clv1-1 cna-1* plant. Note the ectopic flowers in the center of the meristem and the lack of primordia around the periphery.

A606V substitution in *cna-1* (Figure 4C). Some phenotypes of *rev-3* plants are stronger than that of *rev-6* or *rev-8* putative null alleles (Talbert et al., 1995; Otsuga et al., 2001; Figure 4D), suggesting that *rev-3* is also likely a dominant-negative allele.

The dominant-negative character of *cna-1* complicated efforts to confirm gene isolation by complementation. We chose to express *CNA* under the previously characterized regulatory elements from the closely related *REV* gene (P_{REV}) (Zhong and Ye, 1999) because *REV* is expressed in similar tissues to *CNA* (see below) and because we had not identified the *CNA* regulatory sequences. When P_{REV}:*cna-1* was transformed into *clv3-4*, 22 of 77 independent lines exhibited Cna$^-$ phenotypes, including the loss of organogenesis and formation of organs in the center of the meristem (Figure 2L). For P_{REV}:*CNA* transformed into *clv3-4*, only 1 of 45 independent lines displayed Cna$^-$ phenotypes (data not shown). Similar results were observed with smaller numbers of lines with these constructs transformed into *clv3-1* and *clv3-2*, and P_{REV}:*CNA* was unable to complement either *clv3-1 cna-1* or *clv3-2 cna-1* (data not shown).

We assessed *CNA* expression by RNA in situ hybridization (see Supplemental Figure 7 online). Consistent with separate studies, we observed that during embryo development *CNA* expression is strongest in the developing vascular elements and the adaxial portion of cotyledons (Prigge et al., 2005; data not shown). Ohashi-Ito and Fukuda (2003) have also shown that *CNA/ATHB15* is expressed in developing vascular elements using a $P_{CNA/ATHB15}$:β-glucuronidase (*GUS*) reporter construct. In mature plants, *CNA* continues to be strongly expressed in the developing vascular elements. *CNA* is expressed diffusely in young stage flower meristems but becomes enriched in developing stamens and carpels around stage 8. As flowers matured, we observed strong expression of *CNA* within developing ovules, from the earliest stage of ovule development. *CNA* is also expressed within the shoot meristem (see Supplemental Figure 7 online; Prigge et al., 2005; data not shown).

The Effect of *clv* Mutations on *WUS* and *CLV3* Expression

WUS expression is thought to be intimately associated with the presence of stem cells and considered to be an excellent indicator of the capacity of the meristem to maintain a stem cell population. *CLV3* is currently thought to be the best marker for stem cell identity (see Introduction). To better understand the origin of defects occurring in *clv cna* meristems, we assessed the expression of these two key markers of meristem function in *clv* and *clv cna* double mutants. Previous work has shown that *WUS* is normally expressed in a basal subset of cells in the L3 layer, excluding the outermost, or most apical, L3 cells (Mayer et al., 1998; Schoof et al., 2000). This domain of *WUS* expression expands laterally and apically into the uppermost L3 cell layers in *clv3-2* and *clv1-4* meristems (Brand et al., 2000; Schoof et al., 2000).

Table 3. The *cna-1* Allele Is Dominant-Negative

Genotype	Shoot Meristem Size (μm)[a]	Ring Meristem[b]	Loss of Organogenesis[c]	*n*[d]
clv3-2	209 ± 21	0%	0%	20
clv3-2 cna-2/+	228 ± 17	0%	0%	22
clv3-2 cna-1/+	266 ± 23	22%	0%	18
clv3-2 cna-2/cna-2	260 ± 17	17%	0%	24
clv3-2 cna-1/cna-2	441 ± 20	100%	0%	18
clv3-2 cna-1/cna-1	478 ± 19	91%	36%	22

[a] Values represent the mean shoot apical meristem diameter ± standard error of plants collected simultaneously at the onset of bolting (see Methods).
[b] The percentage of plants showing a distinct ring shape to the meristem.
[c] The percentage of plants showing a severe loss of organogenesis.
[d] *n* indicates the number of measurements used to determine size.

We used P_{WUS}:*GUS* and P_{CLV3}:*GUS* transgenic plant lines that have already been characterized and shown to faithfully reflect endogenous gene expression (Lenhard et al., 2002). The characterized transgenic plant lines were crossed to *clv3-2* and *clv3-2 cna-1* plants to assess GUS accumulation in the mutant backgrounds. As a control, we first assayed GUS accumulation in P_{WUS}:*GUS clv3-2* plants. We were surprised to observe a variable, but often dramatic loss of GUS signal in the shoot apical meristems of *clv3-2* seedlings (Figure 5G). No GUS signal was detected in the inflorescence shoot apical meristems of *clv3-2* plants (Figures 6A and 6C). The expression of P_{WUS}:*GUS* continued to be quite strong in both the floral meristems and young lateral shoot meristems of *clv3-2* plants, indicating that the loss of expression was specific to the shoot apical meristem. Equally surprising, we observed a similar downregulation of P_{CLV3}:*GUS* expression in *clv3-2* shoot apical meristems, although it occurred later than the downregulation of P_{WUS}:*GUS* expression (Figures 7A to 7D). Thus, regulatory sequences from two different genes behaved differently in a *clv3-2* background from descriptions in previously published analyses of these genes from several labs (Fletcher et al., 1999; Schoof et al., 2000; Brand et al., 2000, 2002; Lenhard and Laux, 2003). This finding is at odds with the inference that *WUS* is necessary for specifying stem cell fate because *clv3-2* shoot apical meristems continue to act as if they contained stem cells and generate organs for weeks after downregulation of P_{WUS}:*GUS* and P_{CLV3}:*GUS* transgenes. Furthermore, all of the cells of *clv3-2* apices retain morphological characteristics of stem cells and do not display differentiation (Clark et al., 1993, 1995). Note that we did not observe any obvious loss of P_{WUS}:*GUS* or P_{CLV3}:*GUS* signal from the shoot apical meristems of wild-type plants (Figures 6L and 7I).

Given that artifacts can arise from promoter-GUS analysis, we repeated analysis of *WUS* and *CLV3* expression within *clv* mutants by RNA in situ hybridization. Both *WUS* and *CLV3* antisense probes were generated and were hybridized to *clv3-2* and *clv1-4* tissue, respectively. While the phenotype of *clv1-4* mutants is weaker than that of *clv3-2* mutants, we could not look at *CLV3* expression in *clv3-2* plants because the *clv3-2* allele contains a chromosomal rearrangement within the coding sequence (Fletcher et al., 1999). At early stages of shoot apical meristem development, and within lateral shoot and flower meristems at all stages, *WUS* and *CLV3* expression matched that of previous reports (Figures 5 to 7). However, within the *clv3-2* inflorescence shoot apical meristem, *WUS* expression was dramatically reduced and patchy (Figures 6B and 6D). This

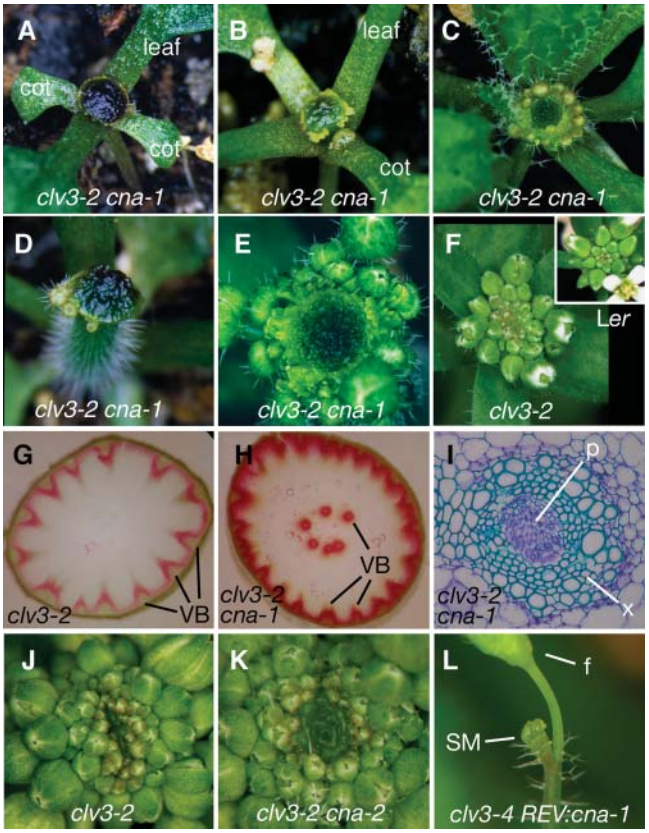

Figure 2. Effects of *cna* Mutations on Organogenesis and Vascular Development.

(A) to **(E)** *clv3-2 cna-1* apices shortly after the transition to flower. Note the variable expressivity in terms of the numbers of leaf and flower organs initiated. cot, cotyledon.
(F) *clv3-2* apex shortly after the transition to flower, with the full complement of leaves and flower primordia apparent. Wild-type L*er* apex shortly after the transition to flowering is shown in the inset.
(G) Phloroglucinol-stained cross section of *clv3-2* inflorescence stem. Note the large number of peripherally located bundles. VB, vascular bundles.
(H) Phloroglucinol-stained cross section of *clv3-2 cna-1* inflorescence stem. Note of the presence of ectopic bundles in the center of the stem. VB, vascular bundle.
(I) High-magnification view of a toluidine-blue stained section of an ectopic internal bundle from a *clv3-2 cna-1* stem. Note the apparent inside-out orientation of the ectopic bundles. x, xylem; p, phloem.
(J) Apex of a *clv3-2* mutant.
(K) Apex of a *clv3-2 cna-2* double mutant.
(L) *clv3-4* single mutant harboring the *REV*:*cna-1* transgene. Note the lack of organ primordia other than a single flower (f). SM, shoot meristem.

Table 4. Effects of *cna-1* on Floral Organ Number in *clv3-2* Mutants

Genotype	Carpels per Flower[a]	P[b]
clv3-2	5.66 ± 0.11 ($n = 59$)	–
clv3-2 cna-1	5.34 ± 0.12 ($n = 67$)	0.04
clv3-2 cna-2	5.79 ± 0.13 ($n = 62$)	0.44

[a] Values represent the mean number of carpels per flower ± standard error. The total number of flowers scored for each genotype is indicated in parentheses (*n*). Only the first 10 flowers of any given plant were included in the analysis.

[b] The probability associated with differences in the mean carpel numbers for *clv3-2* and *clv3-2 cna* lines was assessed using the *t* test.

loss of signal was not the result of experimental anomalies because floral and lateral shoot meristems within the same tissue sections exhibited a strong signal. Expression of *CLV3* within the shoot apical meristems of *clv1-4* plants was not dramatically reduced, although small regions of reduced or absent expression were observed (Figures 7J and 7K). The difference between P_{CLV3}:*GUS* and CLV3 RNA in situ hybridization findings could conceivably result from the smaller meristem sizes of *clv1-4* compared with *clv3-2* or from artifacts of P_{CLV3}:*GUS* transgene activity. In summary, both GUS analysis and RNA in situ hybridizations indicate that *WUS* and possibly *CLV3* expression is lost or reduced from strong *clv* mutants, in contradiction to previous reports.

Whereas *WUS* was not consistently expressed in the region underlying stem cells in *clv3-2* mutants, *WUS* was expressed in several differentiated cells. We detected strong *WUS* signal by RNA in situ hybridization in developing ovules (data not shown), consistent with previously published reports (Groß-Hardt et al., 2002). In addition, we detected *WUS* signal in the developing anther. The earliest anther-specific expression of *WUS* was detected between locules, but later in stamen development *WUS* was detected throughout peripheral anther cells (Figures 6J and 6K).

The Effects of *cna-1* on *WUS* Expression

Despite the unexpected finding that *WUS* and *CLV3* were not appropriate markers for stem cell identity and meristem function within older *clv* shoot meristems, these genes still provided us the best opportunity to assess *clv cna* meristem defects, especially at early stages of development. To this end, we crossed transgenic lines carrying the P_{WUS}:*GUS* or P_{CLV3}:*GUS* construct into the *clv3-2 cna-1* background, and we used antisense *WUS* and *CLV3* probes on *clv3-2 cna-1* tissue in RNA in situ hybridization experiments.

Results from RNA in situ hybridization on embryos indicated that *WUS* expression was unchanged in *clv3-2 cna-1* embryos as compared with *clv3-2* embryos as late as the torpedo stage (Figures 5A and 5B). Within young seedlings, we detected a central gap in *WUS* expression in *clv3-2 cna-1* shoot apical meristems as early as 3 d after germination (Figure 5D), leaving a ring of *WUS* expression around the periphery of *clv3-2 cna-1* apices (Figure 5F).

WUS expression continued to be rapidly lost from *clv3-2 cna-1* shoot apices as they proceeded through development (Figures 5 and 6). There was variability in *WUS* expression patterns and levels, which presumably correlated with the variability of Cna$^-$ phenotypes. A ring of *WUS* expression often persisted on the periphery, even as the rest of the meristem had undergone differentiation (Figures 6E and 6G).

Remarkably, *WUS* expression returned to *clv3-2 cna-1* apices once extensive differentiation occurred. Within *clv3-2 cna-1* inflorescence meristems, small pockets of P_{WUS}:*GUS* expression were observed throughout the apex in what appeared to be differentiated regions, in addition to the expression that persisted on the periphery of the meristem (Figures 6G and 6H). We continued to observe *WUS* expression beyond this stage (data not shown).

The Effects of *cna-1* on *CLV3* Expression

CLV3 is predominantly expressed in the L1 and L2 layers in the center of wild-type meristems (Fletcher et al., 1999; Schoof et al., 2000). As assessed by RNA in situ hybridizations, *CLV3* expression was readily detected in *clv1-4* meristems (Figures 7J and 7K). In *clv3-2 cna-1* double mutants ~12 d old and older, the expression of *CLV3* was quite low and patchy (Figures 7F and 7G). In *clv1-4 cna-1* mutants ~18 d old and older, small pockets of robust *CLV3* expression were observed, especially at the tips of many of the filamentous structures generated during the process of indiscriminate differentiation of the meristem (Figure 7L).

When P_{CLV3}:*GUS* activity was assayed in *clv3-2 cna-1* plants, there was a general trend toward downregulation of *CLV3*

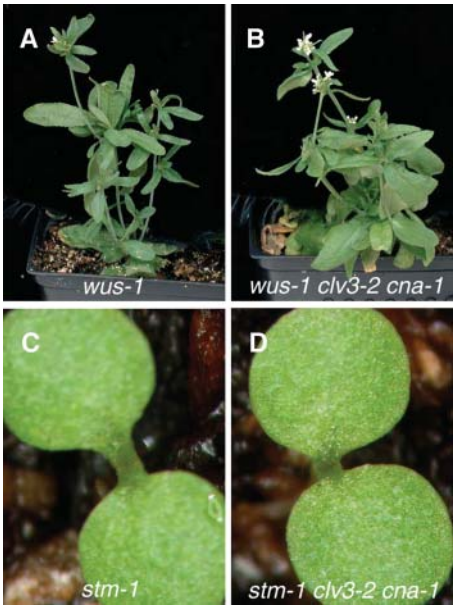

Figure 3. *wus* and *stm* Are Epistatic to *clv3-2 cna-1*.

(A) *wus-1* single mutant.
(B) *wus-1 clv3-2 cna-1* triple mutant.
(C) *stm-1* single mutant.
(D) *stm-1 clv3-2 cna-1* triple mutant.

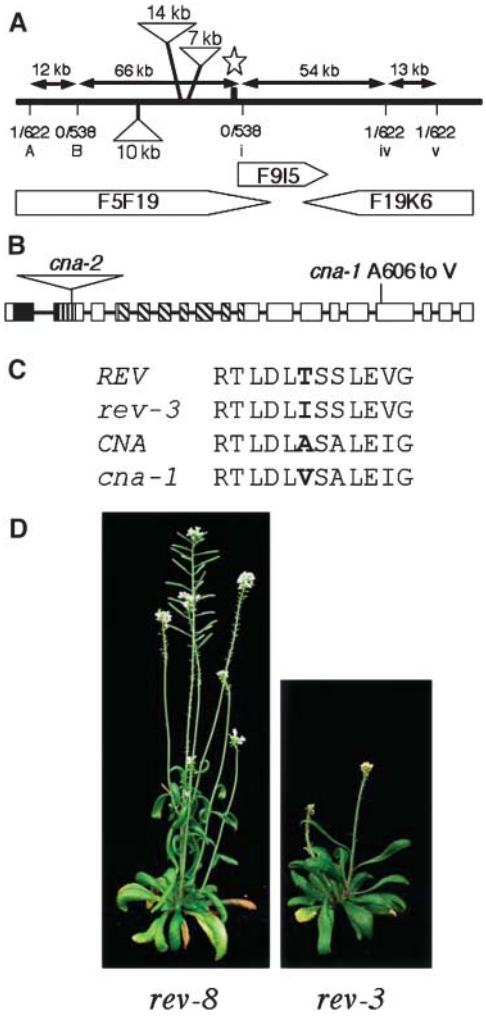

Figure 4. Map-Based Isolation of the *CNA* Gene.

(A) The thick line represents a portion of chromosome I, and the sequenced BAC clones in the region are represented as pentagons. Positions of molecular markers used in fine mapping during the identification of the *CNA* locus (star) are indicated by vertical lines below the chromosome (see Supplemental Table 1 online). The double-headed arrows show the distances between markers in the Landsberg ecotype, and the fractions report the numbers of recombinant chromosomes out of the total number screened in the mapping population. The three triangles indicate the locations of large blocks of sequences present in the Col ecotype but absent in L*er* that appear to be associated with transposon insertions.

(B) Schematic diagram of the *CNA* gene with the positions of the *cna-1* and *cna-2* mutations indicated. Protein-coding exons are indicated by boxes, and introns are indicated by lines. The regions corresponding to the homeodomain, Leu zipper, and START domain are denoted by the solid, vertically hatched, and diagonally hatched boxes, respectively.

(C) Alignment of the sequences around the mutations sites in *rev-3* and *cna-1*. The positions of mutated residues are indicated in bold.

(D) A comparison of the putative null allele *rev-8* and the missense mutant *rev-3*, which exhibits a more severe flower meristem defect.

expression, although both the pattern and loss of expression was more complex than that of P_{WUS}:*GUS*. Similar to *WUS* expression, P_{CLV3}:*GUS* was first reduced in the center of *clv3-2 cna-1* vegetative shoot meristems, although this reduction followed the loss of *WUS* expression by several days (Figures 6 and 7). P_{CLV3}:*GUS* was expressed at low, patchy levels throughout the *clv3-2 cna-1* apex as it underwent differentiation (Figure 7). Older *clv3-2 cna-1* plants exhibited sustained, and later increased, P_{CLV3}:*GUS* expression, especially within the center of the apex, as differentiation proceeded (Figure 7).

The Overlap of *CNA* Function within the HD-Zip III Gene Family

Genetic data suggest the cna-1 protein is dominant-negative and could be interfering with the activity of a functionally redundant protein(s). Because *ATHB8* is the most closely related gene to *CNA* within the Arabidopsis genome, we hypothesized that *ATHB8* might act to replace some of the *CNA* activity in the *clv3-2 cna-2* background. To investigate this possibility, we crossed *clv3-2 cna-2* to *athb8-12*, a T-DNA insertion line in which the T-DNA is located in an intron just upstream of the translation start site (Prigge et al., 2005). The resulting *clv3-2 cna-2 athb8-12* triple mutants did not exhibit enhanced Cna$^-$ phenotypes, suggesting that *ATHB8* does not function in parallel with *CNA* in a *clv3-2* background (data not shown).

We have observed that the *cna-2 phb-13 phv-11* triple null mutant displays an intermediate Clv$^-$ phenotype (Prigge et al., 2005). This suggested that *CNA*, *PHB*, and *PHV* coordinately regulate meristem development. To test this idea of parallel function further and to determine whether the incompletely dominant nature of the *cna-1* allele is due to interference with the normal function of the *PHB* and *PHV* genes, we generated double and triple mutant combinations of *phb* and *phv* null alleles with *cna-1*. We then compared the phenotypes of the *cna-1 phb-13* and *cna-2 phb-13* double mutants and the *cna-1 phb-13 phv-11* and *cna-2 phb-13 phv-11* triple mutants. Because the *cna-2*, *phb-13*, and *phv-11* alleles were all in the Columbia (Col) background, the phenotypes were analyzed after the *cna-1* allele had been introgressed into the Col background by two crosses.

Whereas *cna-2 phb* double mutants exhibit very weak Clv$^-$ phenotypes (Prigge et al., 2005), all *cna-1 phb* plants and most *cna-1*/+ *phb* plants exhibited a brief developmental arrest after germination and expansion of the first two true leaves (Figures 8B and 8C). Organogenesis in the arrested plants resumed 10 to 14 d after germination. Subsequently, the *cna-1 phb* apices exhibited a stronger Clv$^-$ phenotype than *cna-2 phb* apices, developing fasciated stems that frequently bifurcated and flowers with extra carpels. This suggests that *cna-1* may interfere with *PHV* function because similar phenotypes are seen for *cna-2 phb phv* apices (data not shown; Figure 8I; Prigge et al., 2005).

cna-1 phb plants also heterozygous or homozygous for *phv* exhibited early arrest and later recovery as well, with *cna-1 phb phv* individuals among the last to recover (Figure 8D; data not shown). For the shoots that developed after recovery from arrest, the presence of the *cna-1* allele enhanced the *phb* and *phv* alleles to a much greater extent than the likely null *cna-2* allele. Both

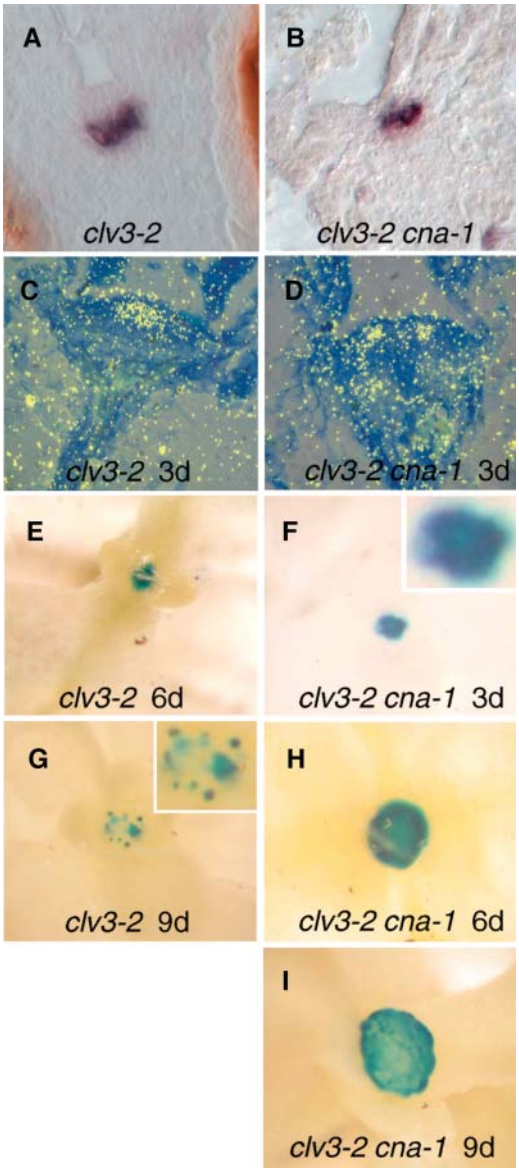

Figure 5. *WUS* Expression in Vegetative Meristems of *clv3-2* and *clv3-2 cna-1* Plants.

(A) and **(B)** *WUS* mRNA was detected in *clv3-2* **(A)** and *clv3-2 cna-1* **(B)** torpedo-stage embryos using dioxygenin-labeled riboprobes. *WUS* signal is indicated by indigo staining.

(C) and **(D)** *WUS* mRNA was detected in 3-d-old *clv3-2* **(C)** and *clv3-2 cna-1* **(D)** seedlings using ^{35}S-labeled riboprobes. *WUS* mRNA signal is shown in yellow. Note the gap in *WUS* signal in the center of the *clv3-2 cna-1* apex.

(E) to **(I)** Detection of P_{WUS}:*GUS* expression in *clv3-2* (**[E]** and **[G]**) and *clv3-2 cna-1* (**[F]**, **[H]**, and **[I]**) seedlings on day 3 **(F)**, day 6 (**[E]** and **[H]**), and day 9 (**[G]** and **[I]**). The blue color indicates tissues with GUS activity. The insets in **(F)** and **(G)** show higher magnification views of the meristems. Note the loss of P_{WUS}:*GUS* signal from the day 9 *clv3-2* sample and the loss of central P_{WUS}:*GUS* signal from the *clv3-2 cna-1* plants as early as day 3.

cna-1 phb phv/+ and *cna-1 phb phv/phv* plants developed massively enlarged shoot meristems (Figure 8E; data not shown) and, in the case of *cna-1 phb phv/phv* plants, radially symmetric leaves in the middle of the massively enlarged meristem (Figures 8E and 8F). When *cna phb phv* triple mutants began producing flowers, very little stem elongation was apparent and the stems were generally wider than they were tall with very disorganized vascular elements (Figures 8F and 8J). Similar to *clv cna* mutants, *cna-1 phb phv* plants exhibited a rapid and total differentiation of the entire massive apex into flowers (Figure 8F). Eventually, secondary inflorescences escaped that elongated normally and developed flowers that were similar in appearance to those of *cna-2 phb phv* triple mutants (Figures 8G and 8I; Prigge et al., 2005). Like *cna-1 clv* apices, the *cna-1 phb phv* primary and secondary meristems frequently exhibited ring-like corona meristems and eventually ceased organ production (Figure 8H; data not shown). *cna-1* displayed dominant-negative characteristics in the *phb phv* background (see Supplemental Table 3 online).

DISCUSSION

We have identified *CNA* as a novel regulator of meristem development. In a *clv* background, mutations within the *CNA* gene led to dramatic defects in meristem size, organogenesis, stem cell maintenance, and the expression of *WUS* and *CLV3*. We propose that CNA acts in parallel with the CLV pathway to promote organ formation. We show that *CNA* corresponds to *ATHB15*, a member of the HD-Zip III gene family, and that *CNA* is expressed strongly within developing vascular elements and diffusely within developing meristems and organ primordia. The putative dominant-negative *cna-1* allele appears to interfere with the function of both HD-Zip III family members as well as other genes. While investigating *CLV3* and *WUS* expression within *clv* and *clv cna* plants, we observed that *WUS* may be neither necessary nor sufficient for stem cell specification and that *CLV3* expression may not be a marker for stem cell identity, in contradiction to the existing paradigm in the field.

cna Alleles and Genetics

The observation that *cna-1* enhanced the phenotypes of *clv1*, *clv2*, and *clv3* mutants, including the *clv3-2* null allele, suggests that *CNA* functions in a pathway parallel to that of the *CLV* loci. The requirement for *CNA* increases as CLV signaling is lost, such that the least apparent *cna* effects were observed in otherwise wild-type backgrounds, and the most dramatic phenotypes were observed within strong *clv* mutant backgrounds.

We conclude that the *cna-1* missense allele is dominant-negative for several reasons. First, *cna-1* exhibited a stronger phenotype than the likely null *cna-2* allele. Second, P_{REV}:*CNA* transformed into *clv3-2 cna-1* did not complement the mutant phenotypes, whereas P_{REV}:*cna-1*, but not P_{REV}:*CNA*, transformed into *clv3-2 CNA* and *clv3-4 CNA* backgrounds recreated the Cna$^-$ phenotype. This suggests that cna-1 interferes with the activity of CNA, in addition to other proteins. Third, the missense mutation within *cna-1* (A608 to V) is located in a position analogous to the missense mutation within *rev-3* (T608 to I), which itself exhibits dominant-negative characteristics.

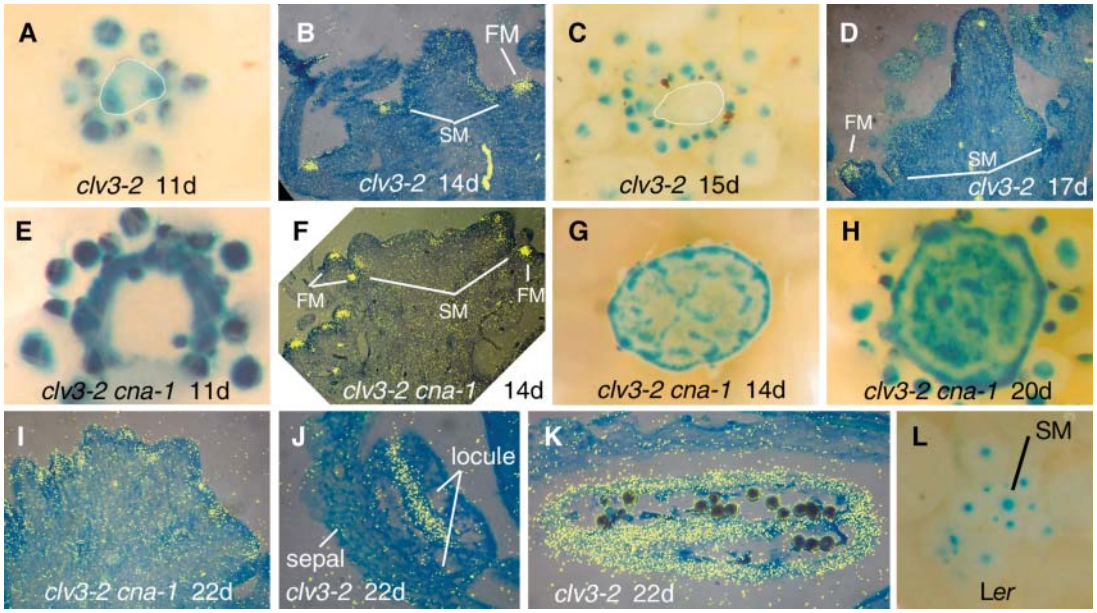

Figure 6. *WUS* Expression in Inflorescences of *clv3-2* and *clv3-2 cna-1* Plants.

Detection of P_{WUS}:*GUS* expression (**[A]**, **[C]**, **[E]**, **[G]**, **[H]**, and **[L]**). Photographs were taken from above the apices, showing GUS activity in blue. Detection of *WUS* mRNA using ^{35}S-labeled probes in longitudinal sections (**[B]**, **[D]**, **[F]**, **[I]**, **[J]**, and **[K]**). *WUS* mRNA signal is shown in yellow. SM, shoot meristem; FM, floral meristem.

(A) The apex of an 11-d-old *clv3-2* plant. The meristem is outlined in white. Note the lack of GUS signal in most of the shoot apical meristem.

(B) The apex of a 14-d-old *clv3-2* plant. Note the robust expression within flower meristems, whereas the shoot apical meristem lacks robust signal.

(C) The apex of a 15-d-old *clv3-2* plant. The meristem is outlined in white.

(D) The apex of a 17-d-old *clv3-2* plant.

(E) The apex of an 11-d-old *clv3-2 cna-1* plant. Note the robust GUS signal around the periphery of the meristem and within the flower meristems both outside and inside the ring. The signal at the bottom of the ring is obscured by a leaf.

(F) The apex of a 14-d-old *clv3-2 cna-1* plant. Note the robust expression within flower meristems, whereas the shoot apical meristem lacks robust signal.

(G) The apex of a 14-d-old *clv3-2 cna-1* plant. Note the ring of GUS signal around the periphery.

(H) The apex of a 20-d-old *clv3-2 cna-1* plant. Note the increase in GUS signal across the center of the apex associated with differentiation.

(I) The apex of a 22-d-old *clv3-2 cna-1* plant. Note the pockets of *WUS* signal.

(J) Developing anther of a 22-d-old *clv3-2* plant.

(K) Older anther of a 22-d-old *clv3-2* plant.

(L) The apex of a wild-type L*er* plant shortly after the transition to flowering.

Interestingly, although *cna-1* and *cna-2* are normally recessive, *cna-1* appears incompletely dominant in the strongest *clv* backgrounds.

We sought to assign a place for *CNA* within the network of meristem regulators and found that both *wus* and *stm* are epistatic to *clv3-2 cna-1*. *WUS* and *STM* are both required for the initiation of shoot meristems. Thus, these epistatic relationships may reflect a role for *CNA* in meristem maintenance, as opposed to meristem initiation. Consistent with this, we see no effect of *cna-1* on the initiation of embryonic shoot meristems, lateral shoot meristems, nor flower meristems.

The Primary Defect in *clv3-2 cna-1* Apices

A key unresolved issue is the primary cause of the complex meristem defects in *clv3-2 cna-1* apices. Although the primary defect(s) in the Cna$^-$ phenotype is not entirely clear, we propose that *CNA* promotes organogenesis in parallel with the CLV pathway. This hypothesis is consistent with many observations. The *cna-1* single mutant has a slightly larger meristem, and *cna-1* enhances the stem cell accumulation defect of weak *clv* mutants. In addition, *cna-1* combined with stronger *clv* alleles leads to the cessation of all organogenesis around the flanks of the meristem. Furthermore, we recently demonstrated that *cna-2 phb phv* triple mutants effectively recreate the Clv$^-$ meristem phenotype (Prigge et al., 2005). The later differentiation of Cna$^-$ apices could be explained if the loss of nascent organ primordia leads to a loss of meristem identity. Classic work has demonstrated that organ primordia influence the positioning of new primordia (Snow and Snow, 1931), as do the central cells of the meristem (Wardlaw, 1949). More recently, clear evidence of the role of polar auxin transport within the meristem in establishing sites of organogenesis has been published (Reinhardt et al., 2000, 2003; Benková et al., 2003). In light of this, we suggest that signaling

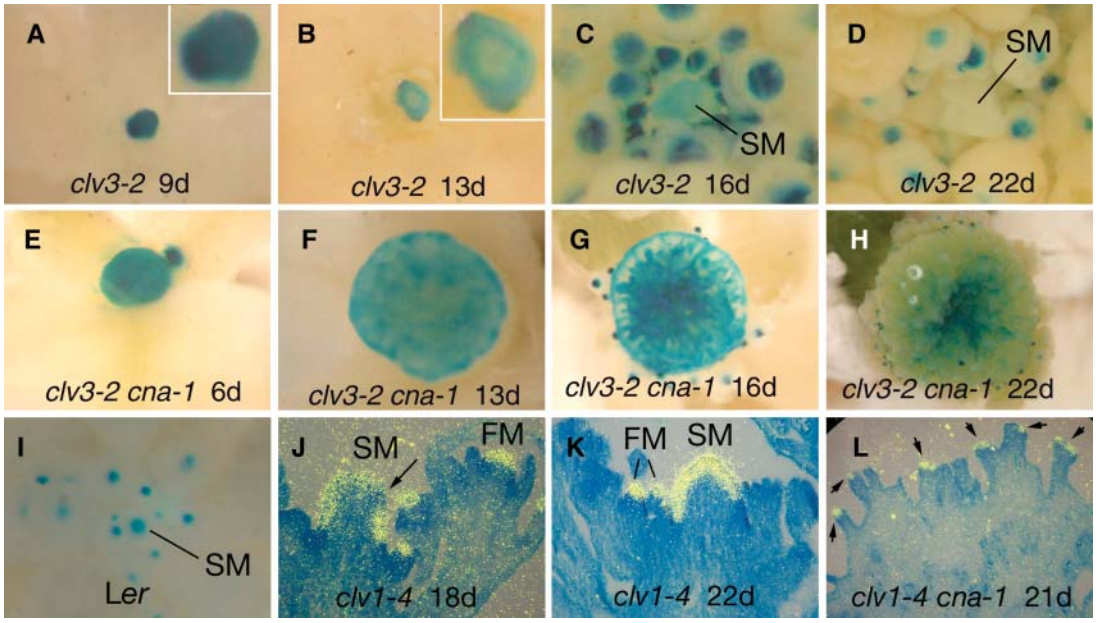

Figure 7. *CLV3* Expression in *clv3-2* and *clv3-2 cna-1* Apices.

Detection of P_{CLV3}:*GUS* expression (**[A]** to **[I]**). Photographs were taken from above the apices, showing GUS activity in blue. Detection of *CLV3* mRNA using ^{35}S-labeled riboprobes in longitudinal sections (**[J]** to **[L]**). *CLV3* signal is shown in yellow. Insets in **(A)** and **(B)** show higher-magnification views of the shoot apical meristem. SM, shoot apical meristem. FM, flower meristem.

(A) The apex of a 9-d-old *clv3-2* plant.

(B) The apex of a 13-d-old *clv3-2* plant. Note that only weak peripheral GUS signal remains.

(C) The apex of a 16-d-old *clv3-2* plant.

(D) The apex of a 22-d-old *clv3-2* plant. Note that the signal is restricted to flower meristems.

(E) The apex of a 6-d-old *clv3-2 cna-1* plant.

(F) The apex of a 13-d-old *clv3-2 cna-1* plant.

(G) The apex of a 16-d-old *clv3-2 cna-1* plant. Note the relative paucity of flower meristems around the periphery.

(H) The apex of a 22-d-old *clv3-2 cna-1* plant. Note the sustained GUS signal in the apex despite the onset of differentiation.

(I) The apex of a wild-type L*er* plant shortly after the transition to flowering.

(J) The apex of an 18-d-old *clv1-4* plant. Note the patch of the shoot apical meristem lacking signal (arrow).

(K) The apex of a 22-d-old *clv1-4* plant.

(L) The apex of a 21-d-old *clv1-4 cna-1* plant. Note the robust *CLV3* signal in the filamentous structures (arrows).

between organ primordia and the center of the meristem is also essential for the maintenance of meristem identity.

cna-1 Dominant-Negative Character

CNA belongs to the HD-Zip class of proteins, first identified by Schena and Davis (1992). HD-Zip III proteins contain a region of similarity to the mammalian sterol/lipid binding domain (START domain), in addition to the N-terminal HD-Zip motif. Most of the C terminus is also well conserved among HD-Zip III proteins, but its function is unknown.

The Arabidopsis HD-Zip III genes have been implicated in the regulation of several developmental processes, including leaf polarity, meristem initiation, and vascular development (Baima et al., 1995, 2001; Talbert et al., 1995; Zhong and Ye, 1999; McConnell et al., 2001; Otsuga et al., 2001; Ohashi-Ito and Fukuda, 2003; Prigge et al., 2005).

We concluded that the *cna-1* allele interferes with the function of other, likely redundant, genes. We hypothesized that other members of the HD-Zip III family were good candidates for *CNA*-redundant genes because extensive functional overlap has been observed between the members of this gene family in several developmental pathways (Emery et al., 2003; Prigge et al., 2005). However, *rev* mutants do not exhibit interactions with *clv* mutants similar to that of *cna* (Otsuga et al., 2001), and we observed no evidence of a role for *ATHB8* in meristem development. Interestingly, we have shown in a separate study that *cna*, *phb*, and *phv* null alleles exhibit functional overlap in meristem development, resulting in a Clv$^-$ phenotype when all three genes are mutated (Prigge et al., 2005). This suggests that these three genes have functional overlap within meristem development and that cna-1 may interfere with the function of PHV and PHB. Indeed, genetic interaction studies of *cna-1* with *phb* and *phv* mutants indicated that *cna-1* interferes with *PHV* function, as well as revealing the ability of these mutations to recreate the Cna$^-$ phenotype in a *CLV*$^+$ genetic background. Because the *cna-1 phb phv* triple mutant also exhibited phenotypes not seen for the *cna-2 phb phv* triple mutant, we predict

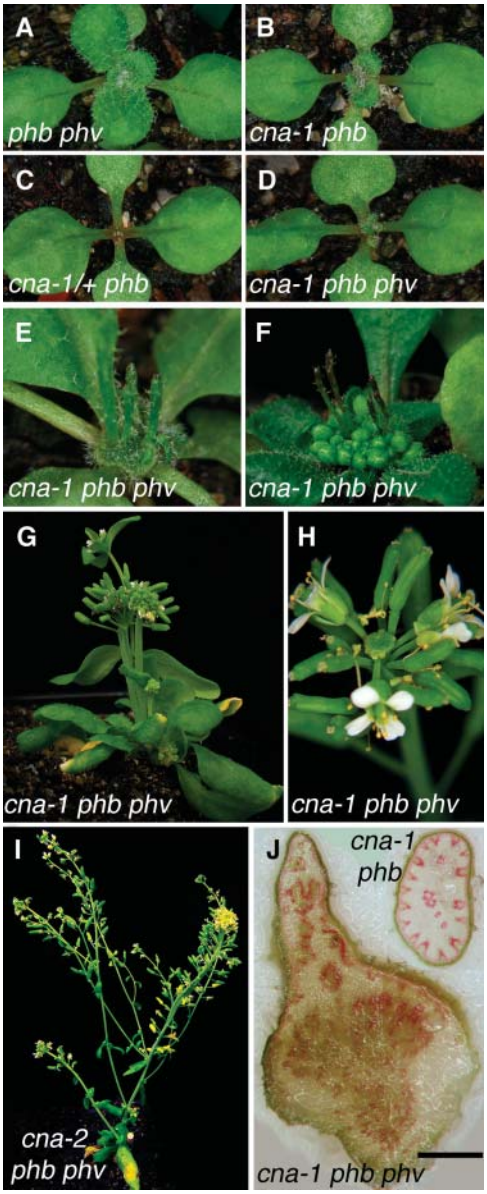

Figure 8. Phenotypes of *cna-1 phb phv* Plants.

(A) A 13-d-old *phb phv* plant was identical in phenotype to wild-type plants.

(B) A 13-d-old *cna-1 phb* plant that underwent only a short developmental arrest.

(C) A 13-d-old *cna-1*/+ *phb* plant with a strong defect in organogenesis.

(D) A 13-d-old *cna-1 phb phv* triple mutant that arrested after the production of two leaves, but then recovered.

(E) A 19-d-old *cna-1 phb phv* seedling with a mass of undifferentiated cells and radially symmetric organs coming from the midst of the meristem.

(F) A *cna-1 phb phv* seedling at day 34. Note the entire apex has differentiated into flowers, but the inflorescence stem did not elongate.

(G) The plant in **(E)** at day 54, with axillary meristems that emerged and elongated relatively normally.

(H) A secondary inflorescence from a 65-d-old *cna-1 phb phv* plant exhibiting a Cna$^-$ phenotype.

that the cna-1 isoform affects additional genes products besides PHB and PHV.

WUS May Not Be Necessary for Stem Cell Specification

An unexpected finding that was born out of the promoter-GUS studies and corroborated by RNA in situ hybridization data was that *clv3-2* shoot apical meristems lose *WUS* expression while maintaining stem cells and organogenesis. The loss of *WUS* expression in the shoot meristem was clearly evident in P_{WUS}:*GUS* assays. RNA in situ hybridization experiments showed a similar downregulation of *WUS*, although there remained patchy and trace expression within the *clv3-2* shoot apical meristems. Both GUS assays and RNA in situ hybridizations revealed that *WUS* expression remains robust within *clv3-2* flower meristems and lateral shoot meristems, despite its apparent loss from the shoot apical meristem.

This loss of *WUS* expression was quite surprising given previous analyses of *clv* phenotypes and *WUS* expression. *clv3-2* shoot apical meristems continue to maintain stem cells and organogenesis late into development, well past the downregulation of *WUS* expression. This raises the question as to how these stem cells are maintained in the absence of *WUS*. Genetic loss of *WUS* function leads to a failure of the *wus* mutant plants to establish stem cell populations at either shoot or flower meristems (Endrizzi et al., 1996; Laux et al., 1996; Mayer et al., 1998), indicating that *WUS* is necessary for stem cell specification. One explanation is that *WUS* is necessary for stem cell initiation but that other factors can redundantly maintain stem cell identity in the absence of *WUS*. Such a *WUS*-independent function might be performed by one of the related *WOX* genes (Haecker et al., 2004).

Harder to resolve is the conflict of some of our observations with previously published data of *WUS* expression in *clv* mutant backgrounds (Brand et al., 2000; Schoof et al., 2000; Lenhard and Laux, 2003). Some of the previous experiments looked at expression in meristems collected relatively early in development. Schoof and coworkers (2000) used vegetative apices and inflorescence apices with age not stated, whereas we observed the greatest *WUS* reduction in later developmental stages. In addition, we grew our samples under significantly higher light levels, which resulted in more robust growth and stronger Clv$^-$ phenotypes. Finally, whereas data from several previous publications revealed that *WUS* expression expands in *clv* mutants, the expression in published images appear somewhat patchy, diffuse, and at a lower levels compared with controls (Brand et al., 2000; Schoof et al., 2000). Moreover, wild-type inflorescence

(I) A 44-d-old *cna-2 phb phv* plant. Note the much weaker phenotypes compared with the *cna-1* triple mutant.

(J) Phloroglucinol-stained hand sections of *cna-1 phb phv* and *cna-1 phb* stems. The unelongated primary inflorescence stems of 54-d-old triple mutants had an unorganized pattern of vascular and lignified tissue (stained pink). The *cna-1 phb* double mutants had relatively normal patterns of lignified cells around the stem periphery, but ectopic vascular bundles appeared in the center of the stem.

meristems in these publications appear to exhibit a weaker *WUS* signal than the vegetative or embryonic meristems.

CLV3 May Not Be a Marker for Stem Cell Function

CLV3 expression may be lost or reduced from the shoot apical meristems of *clv* mutants. The loss of P_{CLV3}:*GUS* expression follows the downregulation observed for *WUS*, consistent with the idea that *WUS* is an activator of *CLV3* expression (Schoof et al., 2000; Brand et al., 2002). Whereas *CLV3* is normally expressed within what appears to be the stem cells of the shoot and floral meristems, in the *clv3-2* mutant background P_{CLV3}:*GUS* assays indicate that *CLV3* expression is lost, even though functional stem cells are presumably maintained at the shoot apical meristem. Whereas some small patches of downregulation of *CLV3* expression were observed in *clv1-4* mutants as determined by RNA in situ hybridization, strong *CLV3* signal was detected across the majority of the *clv1-4* shoot apical meristem. This suggests that either the P_{CLV3}:*GUS* assay overstates the *CLV3* downregulation or that the level reduction depends on the stronger *clv3-2* phenotype. *CLV3* expression is retained normally in *clv* floral meristems and lateral shoot meristems in both assays.

WUS and *CLV3* Can Be Expressed in Differentiated Tissues

WUS and *CLV3* expression have been shown to be largely meristem specific (Mayer et al., 1998; Fletcher et al., 1999; Brand et al., 2000, 2002; Schoof et al., 2000; Lenhard and Laux, 2003). With the exception of *WUS* expression in developing ovules (Groß-Hardt et al., 2002), neither gene has been found to be expressed within differentiated tissue. We show that within the clearly differentiating apices of *clv cna* plants, *WUS* and *CLV3* exhibit strong, stable pockets of expression. Given the absence of convincing markers for differentiated cells, we cannot be sure that the *WUS* and *CLV3* expression in the *clv cna* apices corresponds to fully differentiated cells; however, these cells are very unlikely to be stem cells because they exhibited neither self-renewal nor organogenesis. Thus, in certain genetic backgrounds, one can observe both stem cell function in the possible absence of *WUS* and *CLV3* expression and *WUS* and *CLV3* expression in the apparent absence of stem cells. *WUS* and *CLV3* expression can therefore be uncoupled from stem cell identity. Consistent with this, *WUS* expression is also detected within developing stamens and can be detected by RT-PCR from roots, stems, and leaves (S.-K. Song and S.E. Clark, unpublished data). A key question is why *WUS* and *CLV3* expression within later stage *clv cna* apices is unable to establish stem cells and/or a meristem.

What is clear is the need to identify additional markers for stem cell identity and understand better how *WUS* expression in the organizing center induces stem cell identity within the shoot and flower meristems of wild-type plants.

METHODS

Plant Growth and Mutant Isolation

Plants were grown as described (Yu et al., 2003), except that 0.5 g/pot of Osmocote (Scotts, Marysville, OH) was used and that the plants for Table 3 were grown at 26°C. The isolation of the *cna-1* (formerly known as *pce5*) mutation has been previously described (Pogany et al., 1998). A detailed description of the allele isolation and genetic constructions are presented in the supplemental data online. The isolation of the *cna-2*, *athb8-12*, *phb-13*, and *phv-11* alleles is described elsewhere (Prigge et al., 2005).

Scanning Electron Microscopy Analysis and Meristem Size Estimates

Scanning electron microscopy was performed as described (Dievart et al., 2003). Brightness, contrast, and color balance were adjusted using Adobe Photoshop (Mountain View, CA). For *cna-1* and wild-type meristem sizes, scanning electron micrographs were taken directly above the shoot meristem. A line connecting the ends of the furrow of the youngest stage 1 floral primordium was drawn. The distance from the center of this furrow line perpendicularly across the shoot meristem was determined. This procedure was repeated for the second youngest stage 1 floral primordium. We defined the size of the meristem as the average of these two measurements. For meristem sizes for all other genotypes scanning electron microscopy photographs were taken directly above the shoot meristem, and the center of the meristem was estimated. Both the longest and the shortest diameters across the meristem, going through the center, were used as measurements for each sample.

Stem Cross Sections

Hand-sectioned stems were stained in a solution of 82% ethanol, 14% hydrochloric acid, and 0.09% phloroglucinol (which stains lignin red), for approximately half an hour. Stained sections were photographed immediately using cameras attached to either a Nikon stereomicroscope (transillumination; Tokyo, Japan) or a Zeiss dissecting microscope (epi-illumination; Jena, Germany) (Ruzin, 1999). Stem sections were also fixed, embedded in paraffin, sectioned at 8 μm, and stained with toluidine blue as previously described (Yu et al., 2000).

Molecular Mapping

clv3-2 cna-1 plants were crossed to *er-2* plants in the Col background. DNA was extracted from 311 individual *clv3-2*, *clv3-2 cna-1*/+, and *clv3-2 cna-1*/*cna-1* F2 plants as described (Dellaporta et al., 1983). DNA samples were tested for linkage with published CAPS and simple sequence length polymorphism markers (Konieczny and Ausubel, 1993; Bell and Ecker, 1994) and generated CAPS based on L*er* and Col sequence comparison (Arabidopsis Genome Initiative, 2000; Jander et al., 2002). The F3 seeds collected from individual F2 plants were sown and phenotypically scored to verify the genotype of the F2 parents. Potential candidate genes were amplified and sequenced from *clv3-2 cna-1* and L*er* genomes.

Plant Transformation

The 2.3-kb promoter region upstream of the *REV* transcribed sequence has been previously characterized (Zhong and Ye, 1999). Construction of the pCB321-*REV*:*CNA* plasmid was described (Prigge et al., 2005). The pCB321-*REV*:*cna-1* vector was generated by cutting out a small region of *CNA* cDNA from pCB321-*REV*:*CNA* with *Cla*I and *Nco*I and replacing it with the corresponding region of cDNA from *cna-1* containing the *cna-1* lesion. AGL1 Agrobacteria were transformed with pCB321-P_{REV}:*CNA* and pCB321- P_{REV}:*cna-1*. Plants were agro-transformed by vacuum infiltration (Bechtold and Pelletier, 1998; Clough and Bent, 1998).

GUS Assays

P_{CLV3}:*GUS* (194.3) and P_{WUS}:*GUS* (87.13) lines (Lenhard et al., 2002) were kindly provided by Thomas Laux. GUS staining and fixation were performed as described (Schoof et al., 2000).

RNA in Situ Hybridization

The full-length *CNA* cDNA in the pCRII vector was cut with *Bsp*EI and *Xho*I, treated with Klenow, and religated to delete the highly conserved HD-Zip region. This plasmid, pCRII-situ*CNA*, was digested with *Xba*I and transcribed with SP6 RNA polymerase to generate antisense riboprobe. The sense riboprobe was similarly generated using *Spe*I and T7 RNA polymerase.

Full-length *WUS* cDNA, including a 51-bp poly(A) tail, was kindly provided by Thomas Laux (Mayer et al., 1998). pBSK-*WUS* was digested with *Eco*RI and *Spe*I, deleting the poly(A) tail, and the resulting fragment was inserted into *Eco*RI- and *Spe*I-cleaved pKUT401, a pPZP222-based binary vector (K.U. Torii and S.E. Clark, unpublished data), to generate pKUT421. To synthesize *WUS* antisense riboprobe, this plasmid was digested with *Eco*RI and transcribed with T7 RNA polymerase.

CLV3 full-length cDNA was cloned into pCR2.1 to generate pCR2.1-c*CLV3*. Antisense riboprobe was generated by digesting with *Sac*I and transcribing with T7 polymerase. Sense riboprobe was generated by digesting with *Spe*I and transcribing with SP6 RNA Polymerase.

Tissues for RNA in situ hybridizations were fixed and embedded as described by Clark et al. (1993). A radioactive in situ protocol was followed for the nonembryonic expression studies (Yu et al., 2003). For nonradioactive hybridizations, riboprobes were labeled with digoxigenin according to the manufacturer's instructions (Roche Scientific, Indianapolis, IN). Hybridization and detection were performed as described in a protocol provided by G.N. Drews (University of Utah) (G.N. Drews, personal communication; Jackson, 1991; Klucher et al., 1996), with the following deviation from the protocol: levamisole (1 mM) was added to the Western Blue (Promega, Madison, WI) premix for the color reaction.

The *CNA* genomic sequence (L*er* ecotype) has been deposited with the EMBL/GenBank data libraries under accession number AY902309.

ACKNOWLEDGMENTS

We thank Thomas Laux and the ABRC for providing seeds and plasmids. We thank Joshua Stomel for assistance with the *cna-1* mapping population. This project was supported by National Science Foundation Grant IBN-0131492 to S.E.C. M.J.P. was supported by National Institutes of Health/National Research Service Postdoctoral Fellowship GM20900 to M.J.P., and K.A.G. was supported by the University of Michigan Cellular Biotechnology Training Program (NIH-GM08353).

Received July 19, 2004; accepted December 29, 2004.

REFERENCES

Arabidopsis Genome Initiative (2000). Analysis of the genome sequence of the flowering plant *Arabidopsis thaliana*. Nature **408,** 796–815.

Baima, S., Nobili, F., Sessa, G., Lucchetti, S., Ruberti, I., and Morelli, G. (1995). The expression of the *Athb-8* homeobox gene is restricted to provascular cells in *Arabidopsis thaliana*. Development **121,** 4171–4182.

Baima, S., Possenti, M., Matteucci, A., Wisman, E., Altamura, M.M., Ruberti, I., and Morelli, G. (2001). The Arabidopsis ATHB-8 HD-ZIP protein acts as a differentiation-promoting transcription factor of the vascular meristems. Plant Physiol. **126,** 643–655.

Barton, M.K., and Poethig, R.S. (1993). Formation of the shoot apical meristem in *Arabidopsis thaliana*: An analysis of development in the wild type and *shoot meristemless* mutant. Development **119,** 823–831.

Bechtold, N., and Pelletier, G. (1998). In planta *Agrobacterium*-mediated transformation of adult *Arabidopsis thaliana* plants by vacuum infiltration. Methods. Mol. Biol. **82,** 259–266.

Bell, C.J., and Ecker, J.R. (1994). Assignment of 30 microsatellite loci to the linkage map of *Arabidopsis*. Genomics **19,** 137–144.

Benková, E., Michniewicz, M., Sauer, M., Teichmann, T., Seifertová, D., Jürgens, G., and Friml, J. (2003). Local, efflux-dependent auxin gradients as a common module for plant organ formation. Cell **115,** 591–602.

Brand, U., Fletcher, J.C., Hobe, M., Meyerowitz, E.M., and Simon, R. (2000). Dependence of stem cell fate in *Arabidopsis* on a feedback loop regulated by *CLV3* activity. Science **289,** 617–619.

Brand, U., Grunewald, M., Hobe, M., and Simon, R. (2002). Regulation of *CLV3* expression by two homeobox genes in Arabidopsis. Plant Physiol. **129,** 565–575.

Byrne, M.E., Barley, R., Curtis, M., Arroyo, J.M., Dunham, M., Hudson, A., and Martienssen, R.A. (2000). *ASYMMETRIC LEAVES1* mediates leaf patterning and stem cell function in Arabidopsis. Nature **408,** 967–971.

Byrne, M.E., Simorowski, J., and Martienssen, R.A. (2002). *ASYMMETRIC LEAVES1* reveals *knox* gene redundancy in Arabidopsis. Development **129,** 1957–1965.

Clark, S.E., Jacobsen, S.E., Levin, J., and Meyerowitz, E.M. (1996). The *CLAVATA* and *SHOOTMERISTEMLESS* loci competitively regulate meristem activity in *Arabidopsis*. Development **122,** 1567–1575.

Clark, S.E., Running, M.P., and Meyerowitz, E.M. (1993). *CLAVATA1*, a regulator of meristem and flower development in *Arabidopsis*. Development **119,** 397–418.

Clark, S.E., Running, M.P., and Meyerowitz, E.M. (1995). *CLAVATA3* is a specific regulator of shoot and floral meristem development affecting the same process as *CLAVATA1*. Development **121,** 2057–2067.

Clark, S.E., Williams, R.E., and Meyerowitz, E.M. (1997). The *CLAVATA1* gene encodes a putative receptor kinase that controls shoot and floral meristem size in *Arabidopsis*. Cell **8,** 575–585.

Clough, S.J., and Bent, A.F. (1998). Floral dip: A simplified method for *Agrobacterium*-mediated transformation of *Arabidopsis thaliana*. Plant J. **16,** 735–743.

Dellaporta, S.L., Wood, J., and Hicks, J.B. (1983). A plant DNA minipreparation: Version II. Plant Mol. Biol. Rep. **1,** 19–21.

Dievart, A., Dalal, M., Tax, F.E., Lacey, A.D., Huttly, A., Li, J., and Clark, S.E. (2003). *CLAVATA1* dominant-negative alleles reveal functional overlap between multiple receptor kinases that regulate meristem and organ development. Plant Cell **15,** 1198–1211.

Emery, J.F., Floyd, S.K., Alvarez, J., Eshed, Y., Hawker, N.P., Izhaki, A., Baum, S.F., and Bowman, J.L. (2003). Radial patterning of *Arabidopsis* shoots by class III HD-ZIP and KANADI genes. Curr. Biol. **13,** 1768–1774.

Endrizzi, K., Moussain, B., Haecker, A., Levin, J.Z., and Laux, T. (1996). The *SHOOT MERISTEMLESS* gene is required for maintenance of undifferentiated cells in *Arabidopsis* shoot and floral meristems and acts at a different regulatory level than the meristem genes *WUSCHEL* and *ZWILLE*. Plant J. **10,** 967–979.

Fletcher, J.C., Brand, U., Running, M.P., Simon, R., and Meyerowitz, E.M. (1999). Signaling of cell fate decisions by *CLAVATA3* in *Arabidopsis* shoot meristems. Science **283,** 1911–1914.

Groß-Hardt, R., Lenhard, M., and Laux, T. (2002). *WUSCHEL* signaling functions in interregional communication during *Arabidopsis* ovule development. Genes Dev. **16,** 1129–1138.

Haecker, A., Groß-Hardt, R., Geiges, B., Sarkar, A., Breuninger, H., Herrmann, M., and Laux, T. (2004). Expression dynamics of *WOX* genes mark cell fate decisions during early embryonic patterning in *Arabidopsis thaliana*. Development **131,** 657–668.

Jackson, D. (1991). *In-situ* hybridisation in plants. Molecular Plant Pathology: A Practical Approach, D.J. Bowles, S.J. Gurr, and M. McPherson, eds (Oxford: Oxford University Press), pp. 163–174.

Jander, G., Norris, S.R., Rounsley, S.D., Bush, D.F., Levin, I.M., and Last, R.L. (2002). Arabidopsis map-based cloning in the post-genome era. Plant Physiol. **129,** 440–450.

Jeong, S., Trotochaud, A.E., and Clark, S.E. (1999). The Arabidopsis *CLAVATA2* gene encodes a receptor-like protein required for the stability of the CLAVATA1 receptor-like-kinase. Plant Cell **11,** 1925–1933.

Klucher, M.K., Chow, H., Reiser, L., and Fischer, R.L. (1996). The *AINTEGUMENTA* gene of Arabidopsis required for ovule and female gametophyte development is related to the floral homeotic gene *APETALA2*. Plant Cell **8,** 137–153.

Konieczny, A., and Ausubel, F.M. (1993). A procedure for mapping *Arabidopsis* mutations using co-dominant ecotype-specific PCR-based markers. Plant J. **4,** 403–410.

Laux, T., Mayer, K.F.X., Berger, J., and Jürgens, G. (1996). The *WUSCHEL* gene is required for shoot and floral meristem integrity in *Arabidopsis*. Development **122,** 87–96.

Lenhard, M., Jürgens, G., and Laux, T. (2002). The *WUSCHEL* and *SHOOTMERISTEMLESS* genes fulfill complementary roles in *Arabidopsis* shoot meristem regulation. Development **129,** 3195–3206.

Lenhard, M., and Laux, T. (2003). Stem cell homeostasis in the Arabidopsis shoot meristem is regulated by intercellular movement of CLAVATA3 and its sequestration by CLAVATA1. Development **130,** 3163–3173.

Long, J.A., Moan, E.I., Medford, J.I., and Barton, M.K. (1996). A member of the KNOTTED class of homeodomain proteins encoded by the *STM* gene in *Arabidopsis*. Nature **379,** 66–69.

Lukowitz, W., Gillmore, C.S., and Scheible, W.R. (2000). Positional cloning in Arabidopsis. Why it feels good to have a genome initiative working for you. Plant Physiol. **123,** 796–805.

Mayer, K.F.X., Schoof, H., Haecker, A., Lenhard, M., Jürgens, G., and Laux, T. (1998). Role of *WUSCHEL* in regulating stem cell fate in the *Arabidopsis* shoot meristem. Cell **95,** 805–815.

McConnell, J.R., and Barton, M.K. (1998). Leaf polarity and meristem formation in *Arabidopsis*. Development **125,** 2935–2942.

McConnell, J.R., Emery, J., Eshed, Y., Bao, N., Bowman, J., and Barton, M.K. (2001). Role of *PHABULOSA* and *PHAVOLUTA* in determining radial patterning in shoots. Nature **411,** 709–713.

Ohashi-Ito, K., and Fukuda, H. (2003). HD-Zip III homeobox genes that include a novel member, *ZeHB-13* (*Zinnia*)/*ATHB-15* (*Arabidopsis*), are involved in procambium and xylem cell differentiation. Plant Cell Physiol. **44,** 1350–1358.

Otsuga, D., DeGuzman, B., Prigge, M.J., Drews, G.N., and Clark, S.E. (2001). *REVOLUTA* regulates meristem initiation at lateral positions. Plant J. **25,** 223–236.

Pogany, J.A., Simon, E.J., Katzman, R.B., De Guzman, B.M., Yu, L.P., Trotochaud, A.E., and Clark, S.E. (1998). Identifying novel regulators of shoot meristem development. J. Plant Res. **111,** 307–313.

Prigge, M.J., Otsuga, D., Alonso, J.M., Ecker, J.R., Drews, G.N., and Clark, S.E. (2005). Class III homeodomain-leucine zipper gene family members have overlapping, antagonistic, and distinct roles in Arabidopsis development. Plant Cell **17,** 61–76.

Reinhardt, D., Mandel, T., and Kuhlemeier, C. (2000). Auxin regulates the initiation and radial position of plant lateral organs. Plant Cell **12,** 507–518.

Reinhardt, D., Pesce, E.R., Stieger, P., Mandel, T., Baltensperger, K., Bennett, M., Traas, J., Friml, J., and Kuhlemeier, C. (2003). Regulation of phyllotaxis by polar auxin transport. Nature **426,** 255–260.

Ruzin, S.E. (1999). Plant Microtechnique and Microscopy. (New York: Oxford University Press).

Schena, M., and Davis, R.W. (1992). HD-Zip proteins: Members of an *Arabidopsis* homeodomain protein superfamily. Proc. Natl. Acad. Sci. USA **89,** 3894–3898.

Schoof, H., Lenhard, M., Haecker, A., Mayer, K.F.X., Jürgens, G., and Laux, T. (2000). The stem cell population of *Arabidopsis* shoot meristems is maintained by a regulatory loop between the *CLAVATA* and *WUSCHEL* genes. Cell **100,** 635–644.

Snow, M., and Snow, R. (1931). Experiments on phyllotaxis. I. The effect of isolating a primordium. Philos. Trans. R. Soc. Lond. B Biol. Sci. **221,** 1–43.

Steeves, T.A., and Sussex, I.M. (1989). Patterns in Plant Development. (Cambridge, UK: Cambridge University Press).

Talbert, P.B., Alder, H.T., Parks, D.W., and Comai, L. (1995). The *REVOLUTA* gene is necessary for apical meristem development and for limiting cell divisions in the leaves and stems of *Arabidopsis thaliana*. Development **121,** 2723–2735.

Wardlaw, C.W. (1949). Further experimental observations on the shoot apex of *Dryopteris aristata* Druce. Phil. Trans. R. Soc. Lond. Ser. B **233,** 415–451.

Yu, L.P., Miller, A.K., and Clark, S.E. (2003). *POLTERGEIST* encodes a phosphatase 2C that regulates *CLAVATA* pathways controlling stem cell identity at *Arabidopsis* shoot and flower meristems. Curr. Biol. **13,** 170–188.

Yu, L.P., Simon, E.J., Trotochaud, A.E., and Clark, S.E. (2000). *POLTERGEIST* functions to regulate meristem development downstream of the *CLAVATA* loci. Development **137,** 1661–1670.

Zhong, R., and Ye, Z.-H. (1999). *IFL1*, a gene regulating interfascicular fiber differentiation in Arabidopsis encodes a homeodomain-leucine zipper protein. Plant Cell **11,** 2139–2152.

Zhong, R., and Ye, Z.-H. (2001). Alteration of auxin polar transport in the Arabidopsis *ifl1* mutants. Plant Physiol. **126,** 549–563.